Available online at www.sciencedirect.com
ScienceDirect
Journal of Power Sources 161 (2006) 864–871
JOURNAL OF POWER SOURCES
www.elsevier.com/locate/jpowsour

Investigation on "saw-tooth" behavior of PEM fuel cell performance during shutdown and restart cycles

Zhigang Qi *, Hao Tang, Qunhui Guo, Bin Du

Plug Power Inc., 968 Albany Shaker Road, Latham, NY 12110, USA

Received 21 March 2006; received in revised form 26 April 2006; accepted 27 April 2006
Available online 23 June 2006

Abstract

It was sometimes observed that the performance of a proton-exchange membrane fuel cell improved after the cell went through shutdown and restart cycles. Such a performance recovery led to a "saw-tooth" performance pattern when multiple shutdowns and restarts occurred during the endurance test of a fuel cell. The shutdowns included both planned shutdowns and unintended ones due to station trips or emergency stops (E-stops). The length of the shutdown periods ranged from a few minutes to several weeks. Although such a "saw-tooth" behavior could be attributed to multiple reasons such as: (1) catalyst surface oxidation state change; (2) catalyst surface cleansing; or (3) water management, we found that it was mainly related to water management in our cases after a systematic investigation employing both single cells and stacks.

Keywords: Proton-exchange membrane fuel cell; Performance recovery; Flooding; Catalyst oxidation; Catalyst poisoning; Degradation

1. Introduction

Durability and stability [1,2] are two major performance parameters that will determine the success or failure of a fuel cell system in commercial markets. High durability enables a fuel cell system to operate over long periods without failures, hence minimizing maintenance costs and outages. It could also make the relatively high initial capital investment of a fuel cell system a non-issue because the lifetime cost of ownership of a fuel cell system would be less than that of batteries and other conventional technologies after factoring in the operation and maintenance costs. Multiple approaches should be explored in order to enhance the durability and stability of a fuel cell system. Using more costly components may be one of the short-term solutions, but the initial high cost would impede the acceptance of this technology by the general public.

Stability is reflected by performance degradation, which includes recoverable and unrecoverable modes. Recoverable degradation is caused by temporary and reversible changes in fuel cell performance due to events such as cell flooding, MEA dry-out, catalyst surface oxidation state change, and catalyst surface poisoning. Once these events are corrected, the fuel cell will regain its lost performance. However, if corrective actions are not taken in a timely fashion, these events could cause irreversible damage to a fuel cell. For example, drying could lead to permanent membrane damage, and flooding could accelerate carbon corrosion in the catalyst layer and/or gas diffusion layer (GDL).

An unrecoverable degradation is often caused by permanent changes in the physical properties of one or more fuel cell components. Such changes cannot be undone through corrective actions. Events leading to such irreversible changes include catalyst dissolution and migration [3–5], catalyst sintering [6–9], catalyst surface chemical composition change, carbon oxidation and corrosion [10–12], loss of catalyst–ionomer–reactant three-phase regions, membrane weakening and breech, and delamination of MEA layers. Conditions leading to poor stability will ultimately lead to low durability.

At the same time, good stability makes the control and operation of a fuel cell system easier and user-friendlier. Poor stability creates extra challenges in fuel cell system design and control. For example, if fuel cell performance fluctuates over a wide range, it could reach operating limits and trigger an unplanned system shutdown. Uncontrolled shutdown and restart of a fuel cell is known to seriously damage a carbon-supported cathode

* Corresponding author. Tel.: +1 518 738 0229; fax: +1 518 782 7914.
E-mail address: zhigang_qi@plugpower.com (Z. Qi).

0378-7753/$ – see front matter © 2006 Elsevier B.V. All rights reserved.
doi:10.1016/j.jpowsour.2006.04.137

catalyst due to the formation of an air/fuel boundary at the anode side [13–17]. Even if a performance fluctuation is not large enough to trigger a fuel cell system to shut down suddenly, it could still put extra "stress" on the system because the latter and its components will be in a frequently changing mode to counteract the fluctuation. This could lead the system into a vicious cycle and eventually cause it to spiral out of control, and finally cause the system to shut down.

This article reports a study on a "saw-tooth" behavior that is related to fuel cell stability and performance recovery. This behavior was observed during fuel cell system shutdown and restart cycles.

2. Experimental

2.1. Fuel cell tests

Fuel cell tests were conducted using single fuel cells (50 cm^2 active area), stacks, and systems (~250 cm^2 active area). The single cell test fixture was composed of a pair of graphite plates with single serpentine flow-fields for the reactants. There was a cooling channel on the back of each plate and deionized water at a pre-set temperature was circulated as coolant. In addition, rod-shaped electric heaters were inserted into the plates to provide additional control of the cell temperature.

The stacks consisted of multiple cells, ranging in number from 8 to over 100. Bipolar plates in the stacks were made from graphite composite materials. A liquid coolant was used to control the stack temperature to prevent over heating and to control the stack temperature gradient for water management. For example, by lowering the coolant flow rate, the temperature difference between the coolant outlet and inlet regions is increased. This results in increased water removal via vaporization from both the fuel cell anode and cathode compartments.

In single cell and stack tests, premixed fuel gases and air were used as the reactants at the anode and cathode, respectively. Whenever applicable, a 2% air bleed was used at the anode side to enhance the CO tolerance [18]. The premixed gas was composed of 10 ppm CO, 49% H_2, 17% CO_2; the balance was N_2. In the system tests, reformate was used as the fuel and it was generated *in situ* using an autothermal reforming technique. It contained less than 30 ppm CO, about 40% H_2 (on dry basis), 15–18% CO_2, and the balance was N_2.

Unless otherwise stated, all reactants were preconditioned to 100% relative humidity (RH). The hydrogen/oxygen stoichiometry was set at 1.2/2.0, respectively. Cell temperature was maintained at 65 °C. For stacks and systems, cell temperature refers to the coolant inlet temperature.

Commercial MEAs were used for all the tests. The MEAs were designed for operation with fully humidified reactants in order to achieve long operating hours. Pt–Ru/C and Pt/C were used as the anode and cathode catalysts, respectively. The total Pt loading was less than 1.0 mg cm^{-2}. Perfluorinated ionomer was used as the membrane material, and the thickness of the membrane was less than 30 μm to facilitate water transport across the membrane, to reduce the materials cost, and to improve fuel cell performance.

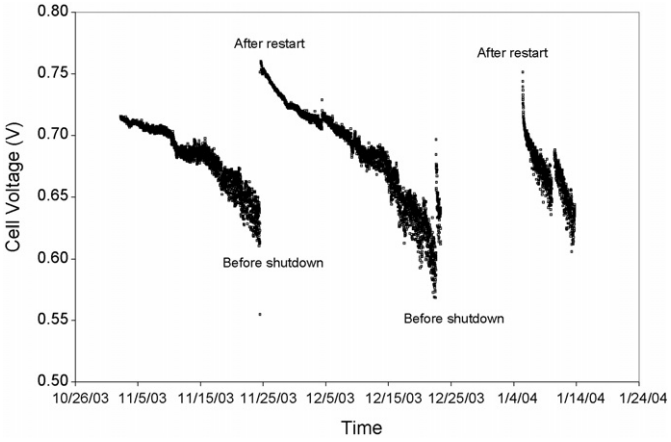

Fig. 1. Performance before shutdowns and after restarts of an aged single cell that had been previously tested for about 2000 h. Premixed fuel gas with 10 ppm CO, 49% H_2, 17% CO_2, balanced by N_2; 1.2/2.0 hydrogen/air stoichiometry; 100% RH; 65 °C cell temperature; 2% air bleed.

3. Results and discussion

3.1. "Saw-tooth" behavior

Fig. 1 shows the voltage versus time plot of a single cell that had been run for several thousand hours before being shut down. The cell was shut down for a very short time on 25 November 2003, and when it was restarted the performance jumped to 0.75 from 0.62 V under the same testing conditions. The cell voltage then gradually declined over time. The cell was again shut down on 23 December 2003; when the cell was restarted on 6 January 2004, its performance again jumped to 0.75 from 0.64 V. Since the cell did not behave like this at the beginning-of-life, some irreversible changes must have happened to it during the endurance test.

Similar behavior was also observed during stack and system operations. Fig. 2 shows several shutdowns and restarts of a fuel cell system operated in the field; the average cell voltage is shown on the *Y*-axis. The stack consisted of about 100 cells with an active area of 250 cm^2 per cell. A substantial voltage increase was seen after each shutdown and restart cycle.

In both Figs. 1 and 2, the performance increase after the shutdown and restart cycles forms a "saw-tooth" pattern on the fuel cell performance versus time chart.

3.2. Hypotheses

There are several plausible mechanisms that could lead to the "saw-tooth" phenomenon. The most likely ones are: (1) catalyst surface oxidation state change, (2) catalyst surface self-cleansing, and (3) water management. These are discussed in the following sections.

3.2.1. Hypothesis 1 — catalyst surface oxidation state change

The catalyst surface, especially at the cathode side, could be subject to oxidation under certain fuel cell operation conditions because of the (high) cathode potential and the presence of water

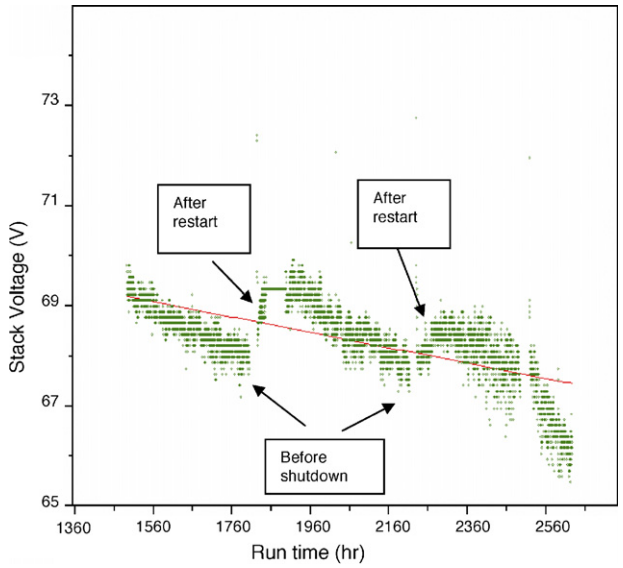

Fig. 2. Performance before shutdowns and after restarts of a fuel cell system during the time interval between 1500 and 2600 h. Reformate that was generated *in situ* using an autothermal reforming technique contained less than 30 ppm CO, about 40% H_2 (on dry basis), 15–18% CO_2, and the balance was N_2. 65 °C coolant inlet temperature; 2% air bleed.

and air [19–23] (Eqs. (1) and (2)):

$$Pt + xH_2O \rightarrow PtO_x + 2xH^+ + 2xe^- \quad (1)$$

$$Pt + 1/2O_2 + H^+ + e^- \rightarrow PtOH \quad (2)$$

For example, the surface of a Pt particle could be oxidized to PtO_x under open circuit voltage (OCV) and to PtOH in fuel cell mode. Both oxidation products are less active towards the oxygen reduction reaction (ORR) than metallic Pt, which is then manifested as an increase in cathode overpotential and a reduction in fuel cell performance.

After a fuel cell is shut down, OCV will gradually decrease from ~1 V to near 0 V as both H_2 and O_2 are consumed through gas crossover and other mechanisms. There are two scenarios to lead to 0 V OCV. The first one is that the air at the cathode side is completely consumed by hydrogen, resulting in H_2/H_2 at anode/cathode. The individual potential at both the anode and cathode is near 0 V. Keeping hydrogen flow while shutting down air flow will be certainly to lead to this scenario. This will enable both PtO_x and PtOH to be reduced back to the more active Pt form. When the fuel cell is restarted, an increase in cell voltage is then achieved because the cathode contains little or no PtOH and PtO_x. As the fuel cell operates, PtO_x and PtOH again gradually build up on the Pt surfaces, which lead to a gradual cell voltage decline. The Pt surface is reactivated once the fuel cell undergoes another shutdown–restart cycle. This performance behavior is consistent with the observed "saw-tooth" phenomenon.

The second scenario is that the remaining hydrogen at the anode side is completely consumed by air, resulting in air/air at anode/cathode. The individual potential at both the anode and cathode is near 1 V, although the OCV is 0 V. Keeping air flow while shutting down hydrogen flow will be certainly to lead to this scenario. This will not lead to the reduction of PtO_x to Pt, but it could help cleanse the electrode surfaces, as discussed below.

3.2.2. Hypothesis 2 — catalyst surface cleaning

The surface of a catalyst must be free of contaminants in order to maintain its high catalytic activity. If an adsorbent covers all or part of this surface, its catalytic activity will decrease because of the reduced accessibility to reactants. Common adsorbents on a Pt electrode include CO, NO_x, SO_x, H_2S, and hydrocarbons [24–29]. During the operation of a fuel cell, the air filter may not be able to completely prevent contaminants from entering the cathode compartment, and these contaminants would accumulate over time on the Pt surface. It is also possible that some adsorbents are generated from the components used in a fuel cell system. This could lead to a continuous decline of available Pt surface area and reduced cathode activity, which is reflected by a gradual voltage decline.

During shutdown and restart, a fuel cell will experience a period of OCV and the cathode potential can be close to 1 V under H_2/air condition. Even the OCV is near 0 V, the cathode potential itself could be also close to 1 V as discussed above. This is high enough to oxidize many adsorbents listed above under air/air condition. With the Pt surface "cleaned", a restarted fuel cell is revitalized and its voltage becomes greater than that just before it was shutdown. The above process would also be consistent with the observed "saw-tooth" phenomenon.

3.2.3. Hypothesis 3 — water management

Water plays an important role in the proper function of a fuel cell [30–33]. A PEM fuel cell generates water at the cathode as part of the electrochemical process. As stated earlier, it requires proper hydration of its membrane electrolyte for adequate proton transport. Most commercial MEAs require the use of humidified fuel/air gas feeds at or near 100% RH. If the amount of water removed is less than that introduced plus produced, flooding will occur within the catalyst layers, GDLs, the flow-fields, and the gas manifolds. The situation can worsen with time, especially in a stack or a single cell with multi-channel flow-fields where gas flows will take the less resistive paths rather than the blocked ones. This would lead to a gradual performance decline that accelerates over time as certain active areas and/or cells become non-functioning. Localized flooding could still exist even if the overall system maintains proper water balance.

Another contribution to flooding could be the aging of cell components over time. For example, one aging result can be the decrease in hydrophobicity of GDL and the carbon catalyst-support in electrodes due to the oxidation of their surfaces during the operation of a fuel cell (Eq. (3)) [12]:

$$C_x + H_2O \rightarrow C_x\text{–}OH + H^+ + e^- \quad (3)$$

This reaction is catalyzed by Pt and occurs at a low oxidation potential [10,11]. Under normal fuel cell operating conditions, this process is not significant because of its sluggish kinetics. When flooding occurs, however, it could potentially lead to local fuel starvation on the anode side. With insufficient fuel supply, the most vulnerable components within the cell, such as carbon, may be oxidized in order to sustain the current demand.

Hydrophobicity loss is also possible if a water-repelling agent such as polytetrafluoroethylene (PTFE) physically segregates from other components within the catalyst layers and the GDLs. Aging could also change the surface properties of the bipolar plates, possibly increasing the resistance to water removal from the flow-fields.

A relationship between the performance recovery after shutdown/restart cycles and flooding may seem not obvious. However, a closer examination suggests that there could be reasonable links. Normally, after a fuel cell is shut down, the load is removed but the reactant gases are still kept flowing through the cell for a short while. Similarly, when a fuel cell is restarted, the reactant gases are first flowed through the cell during the cell warm-up period before any load is applied. Under these conditions, a fuel cell has gas flows but no water production from the electrochemical process. These reactant flows in effect act as a purging force, albeit at a slower flow rate than a typical purging process, but they often last much longer. Thus, it would achieve a similar effect as a purging process, removing part or all of the excess water that had accumulated during the last fuel cell run. This would conceivably lead to the recovery of some or all of the lost fuel cell performance.

In contrast, if the imbalance of water results in excessive removal of water, it would result in gradual dehydration of the ionomer within the catalyst layers and/or the membrane. The situation would worsen with time, leading to a continuous and accelerated decline in performance due to increased ionic resistance. In addition, when there is not enough water within the catalyst layers, the electrochemical reactions would be hampered by the poor proton transport process [34,35]. Although it is highly unlikely that the shutdown and restart processes can hydrate MEAs better than during fuel cell operation, it may be possible that during the shutdown period, water within the fuel cell redistributes itself and moves from the less effective regions to the more effective regions, or moves from locally flooded areas to locally dried areas, resulting in higher performance after the fuel cell is restarted. For example, for a stack with reactant co-flows, the fuel/air inlet regions of a fuel cell may contain less water than the regions near the reactant outlets. The excess water at outlet regions could redistribute itself into the drier inlet regions during the shutdown period.

So, flooding and water redistribution could also lead to the observed "saw-tooth" phenomenon.

3.3. Tests

Experiments were designed and performed in an attempt to differentiate each of the three hypotheses and to identify the actual cause or causes. If the correct root cause(s) is identified, it should enable an operator to turn the "saw-tooth" behavior on and off at will. This would serve as the ultimate proof of the underlining "saw-tooth" mechanism.

3.3.1. Testing hypotheses 1 and 2

Cell potentials were controlled at either near 1 or 0 V in order to evaluate hypotheses 1 and 2. Fig. 3a shows the performance of a cell that had been running at 0.6 A cm^{-2} (cell voltage around

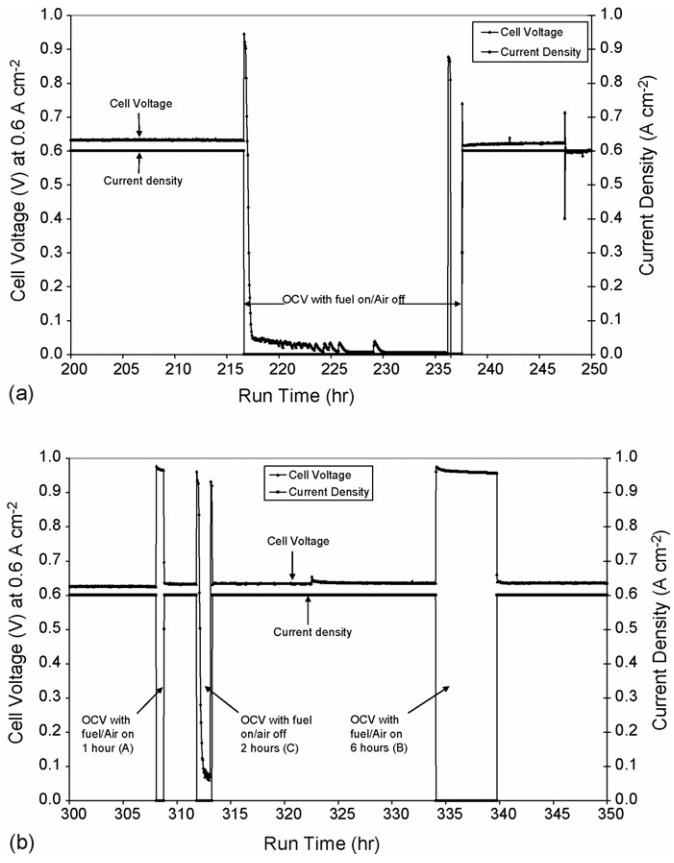

Fig. 3. (a) Effect of low cell voltage (nearly 0 V) on single cell restart performance. (b) Effect of high (0.96 V) and low cell voltage (0.07 V) on restart performance. Premixed fuel gas with 10 ppm CO, 49% H_2, 17% CO_2, balanced by N_2; 1.2/2.0 hydrogen/air stoichiometry; 100% RH; 60 °C cell temperature; 2% air bleed; 0.6 A cm^{-2} load.

0.64 V) for 217 h and then stopped through an E-stop. The air flow at the cathode side was turned off for 20 h while hydrogen was kept flowing at the anode side. The cell voltage quickly declined to nearly 0 V and stayed there for the remainder of the 20 h. Since the air was turned off while the hydrogen was kept flowing, some hydrogen was expected to diffuse through the membrane to the cathode side to consume the remaining air. As the air concentration decreased, the cell open circuit voltage declined. After the OCV became low enough, PtO_x would be reduced to Pt form. In addition, after all the air was consumed by hydrogen, there would be excess hydrogen at the cathode side that could also result in the reduction of PtO_x. After the cell was restarted and air flowed into the cathode side, no apparent performance change was observed before and after this process.

Fig. 3b shows three shutdown/restart cycles. Air flow was maintained during the shutdown at time 307 (region A) and 334 (region B) for 1 and 6 h, respectively. The cell voltage was close to 0.98 V throughout both of the shutdown periods. The cell did gain about a 10 mV performance after the shutdown/restart cycle in region A, which could point to an OCV cleansing effect (hypothesis 2). However, a repeat test in region B under the same condition (except for longer time) did not show any gain in the fuel cell performance. So the 10 mV gain in region A was most

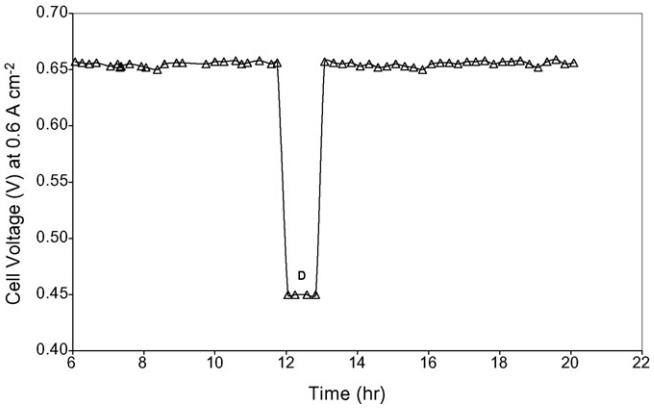

Fig. 4. Effect of low cell voltage (0.45 V) on single cell restart performance. Premixed fuel gas with 10 ppm CO, 49% H_2, 17% CO_2, balanced by N_2; 1.2/2.0 hydrogen/air stoichiometry; 100% RH; 65 °C cell temperature; 2% air bleed; 0.6 A cm^{-2} load.

likely to be due to other reasons. On the other hand, air flow was shut off during the shutdown at time 312 for 2 h (region C), and the cell voltage promptly declined to less than 0.1 V. No apparent performance change was observed after this shutdown and restart cycle.

Fig. 4 shows a different controlled potential experiment. After the cell was operated at 0.6 A cm^{-2} (cell voltage was approximately 0.66 V) for 5 h with 7 °C sub-saturated gas flows, the load was removed, and air was replaced by nitrogen at the cathode side. The cathode potential was then maintained at 0.45 V for 1 h using a Potentiostat (region D). A small amount of air was bled into the cathode side during this process. Since we observed the "saw-tooth" behavior at a cell potential around 0.66 V, we could assume that a potential of 0.66 V was high enough to cause some Pt oxidation in order to avoid the risk by directly eliminating hypothesis 1. It was quite certain that a potential of 0.45 V would be low enough to reduce any PtO_x formed during the cell operation back to Pt. When the fuel cell was restarted, no apparent performance change was observed.

Those results support neither the cathode catalyst surface adsorbent hypothesis nor the cathode catalyst oxidation state change hypothesis. Cell performance did not increase after a restart, and then gradually decrease to pre-shutdown levels, as expected from data similar to that in Figs. 1 and 2.

3.3.2. *Testing hypothesis 3*

In order to test this hypothesis, the inlet reactant humidity level was carefully controlled to simulate flooding as well as a dry/wet cycling situation. Fig. 5a shows the "saw-tooth" behavior of an aged single cell after shutdown/restart cycles when the reactant RH was set to 100%. The cell was then tested for another 5 h with the reactants being 7 °C subsaturated (Fig. 5b). When the cell was restarted after 10 h of shutdown, its performance was similar to that before shutdown. It can also be seen that the cell performed slightly better at 7 °C subsaturation (0.655 V) than at full saturation (0.645 V, Fig. 5a). These experimental results were consistent with the hypothesis that the transition from flooding to a less or no flooding state was the root cause of the "saw-tooth" behavior displayed in Fig. 5a.

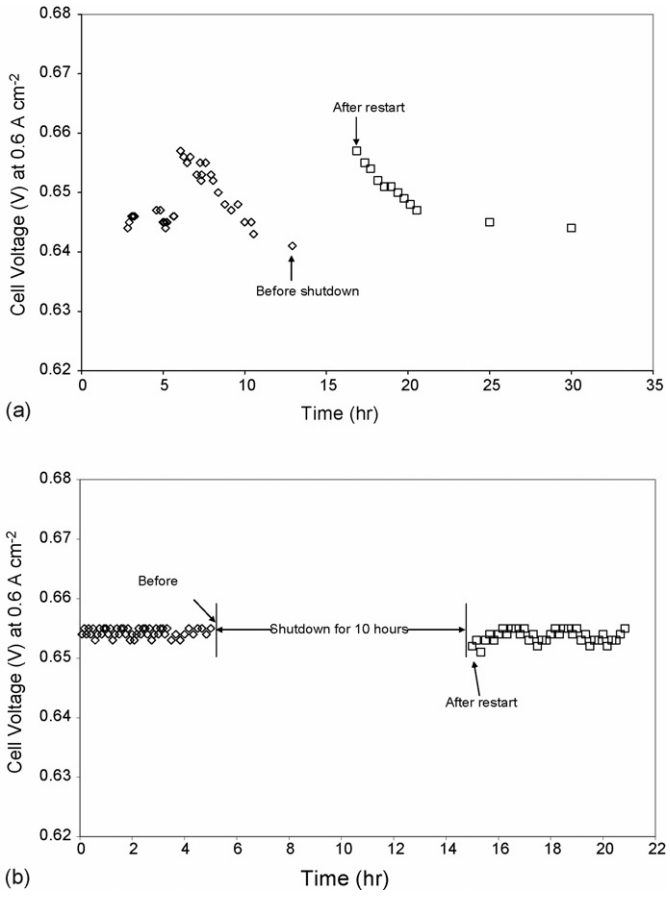

Fig. 5. Effect of reactant humidification on single cell restart performance: (a) full humidification; (b) 7 °C subsaturation. Premixed fuel gas with 10 ppm CO, 49% H_2, 17% CO_2, balanced by N_2; 1.2/2.0 hydrogen/air stoichiometry; 65 °C cell temperature; 2% air bleed; 0.6 A cm^{-2} load.

To further explore the flooding and "saw-tooth" relationship, an eight-cell short stack (module) was built and tested. Fig. 6 shows the maximum, minimum, and average cell voltages of the short stack. When the reactants were fully humidified (e.g., 100% RH), the minimum cell voltage declined quickly and, when it reached 0.3 V, it caused the test station to trip off

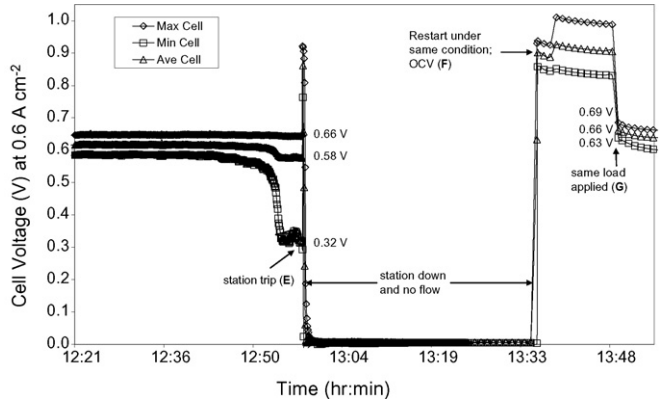

Fig. 6. Performance before shutdown and after restart of an eight-cell module when operated with saturated reactants. Premixed fuel gas with 10 ppm CO, 49% H_2, 17% CO_2, balanced by N_2; 1.2/2.0 hydrogen/air stoichiometry; 65 °C coolant inlet temperature; 2% air bleed; 0.6 A cm^{-2} load.

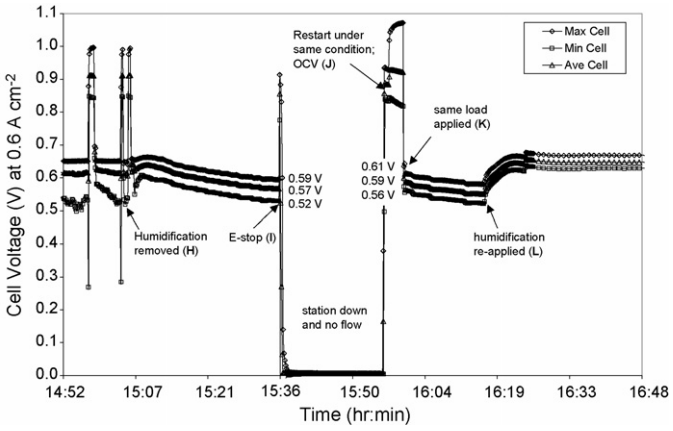

Fig. 7. Performance before shutdown and after restart of an eight-cell module when humidifiers were completely turned off for ca. 30 min. Premixed fuel gas with 10 ppm CO, 49% H_2, 17% CO_2, balanced by N_2; 1.2/2.0 hydrogen/air stoichiometry; 65 °C coolant inlet temperature; 2% air bleed; 0.6 A cm^{-2} load.

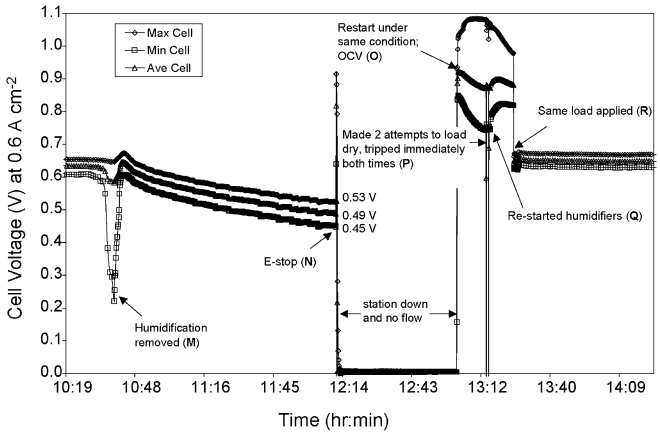

Fig. 8. Performance before shutdown and after restart of an eight-cell module when humidifiers were completely turned off for ca. 90 min. Premixed fuel gas with 10 ppm CO, 49% H_2, 17% CO_2, balanced by N_2; 1.2/2.0 hydrogen/air stoichiometry; 65 °C coolant inlet temperature; 2% air bleed; 0.6 A cm^{-2} load.

(point E). After the station trip, the flows of both reactants were stopped. When the station was restarted after 40 min (point F), the module was kept at the OCV condition with anode and cathode reactants flowing for 12 min before the load was applied (point G). The voltages of all three cells improved, with the minimum cell voltage increasing the most, from 0.32 to 0.63 V.

As seen in Fig. 7 for the same module, the humidification of the reactants was stopped (point H) after the minimum cell tripped the station. The voltage spikes seen around point H were because the module was in the OCV state. In response to the RH reduction, the voltages of all three cells increased initially but they all eventually began to decline. The decline rates were similar among all the cells, and the minimum cell did not show a sudden drop in performance, in contrast to the previous experiment with 100% RH reactants shown in Fig. 6. The station was shut down after about 30 min of testing without humidification (point I). The test was restarted after 20 min, and the load was reapplied after 4 min at OCV. All three cells showed slightly higher performance than that before the shutdown (0.56 V versus 0.52 V; 0.59 V versus 0.57 V; and 0.61 V versus 0.59 V), but the differences were much less significant than those observed in Fig. 6.

In order to completely turn off the "saw-tooth" behavior, the module was operated under a drying condition for a longer time as illustrated in Fig. 8. The humidification of the reactants was turned off before the minimum cell could trip the station (point M), and the module was operated without humidification for about 90 min. Following the initial voltage increase, continuous voltage decline was observed during this period. The station was shut down (point N) for 48 min and then restarted (point O). Reloading the module was attempted twice after 13 min at OCV with unhumidified reactant flows (point P), but the module could not take any load and the station was immediately tripped both times. It was apparent that drying a stack not only turned off the "saw-tooth" behavior, but it also made it impossible to reload the stack. Fully humidified reactants were re-introduced (point Q) for 10 min before reloading the module again. The module was successfully loaded (point R), and the performance was higher than that before the shutdown (0.65 V versus 0.45 V; 0.66 V versus 0.49 V; and 0.67 V versus 0.53 V), presumably due to rehydration of the MEAs.

Based on the fact that the "saw-tooth" behavior could only be turned on and off by changing reactant humidification, it was concluded that the "saw-tooth" phenomenon was directly related to the water management of the fuel cell. It is believed that the cell was in a flooding state before its shutdown, and the reactant flow during the shutdown and restart processes removed some of the excess water, and thus the fuel cell regained its performance after the restart.

MEA flooding can be assessed by electrochemical impedance spectroscopy (EIS). Electrochemical impedance spectra were obtained from the aged cell used to generate the data in Fig. 5a and b and is shown in Fig. 9. Each of the three spectra consists of two semicircles. The semicircles in the low frequency region represent the mass transport resistance. The mass transport resistance was larger with fully humidified reactants (curves *S* and *U*) than that with 7 °C subsaturated reactants (curve *T*).

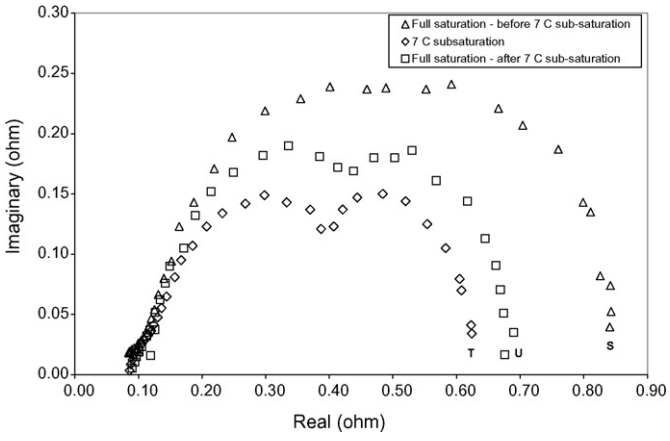

Fig. 9. Electrochemical impedance spectra of an aged cell before, during, and after operation at 7 °C subsaturation. Premixed fuel gas with 10 ppm CO, 49% H_2, 17% CO_2, balanced by N_2; 1.2/2.0 hydrogen/air stoichiometry; 65 °C cell temperature; 2% air bleed; 0.6 A cm^{-2} load.

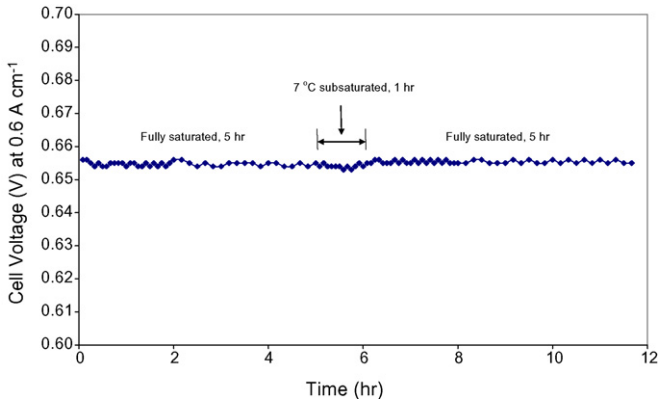

Fig. 10. Effect of 7 °C subsaturation on performance of a new single cell. Premixed fuel gas with 10 ppm CO, 49% H_2, 17% CO_2, balanced by N_2; 1.2/2.0 hydrogen/air stoichiometry; 65 °C cell temperature; 2% air bleed; 0.6 A cm^{-2} load.

This could be indicative of a flooding state when the cell was operated with fully humidified reactants. After running the cell at 7 °C subsaturation for some time, it was then returned to the fully saturated condition. The mass transport resistance (curve *U*) increased but was still significantly less than the initial mass transport resistance taken under fully saturated condition (curve *S*). This indicated that the initial flooding condition was lessened after running the cell at the subsaturation condition, presumably through the removal of the excess water.

It was also found that a new cell was less likely to exhibit the "saw-tooth" pattern than an aged cell. Shown in Figs. 10 and 11, a new cell was subject to shutdown and restart cycles but it did not display the "saw-tooth" behavior. The cell's sensitivity to RH changes was tested by varying the reactant humidification levels.

Fig. 10 shows the performance of the new cell at both fully saturated and 7 °C subsaturated conditions. The performance did not show any noticeable change during and after the 1-h 7 °C subsaturation operation. Fig. 11 compares the performance at different cathode stoichiometry while the reactants were fully saturated. When the cathode stoichiometry was increased from 2.0 to 4.0, the performance jumped from 0.657 to 0.704 V. It then declined to 0.698 V within 1 h of starting the 4.0× air stoichiometry. When the air stoichiometry was reduced from 4.0 to 2.0, the cell voltage declined to 0.648 V, lower than the initial 0.657 V observed prior to the air stoichiometry increase. It then quickly recovered to 0.655 V within 10 min. This demonstrated that a new cell was not sensitive to the controlled variation of the reactant humidification levels. In other words, a new cell has higher tolerance to flooding or drying conditions.

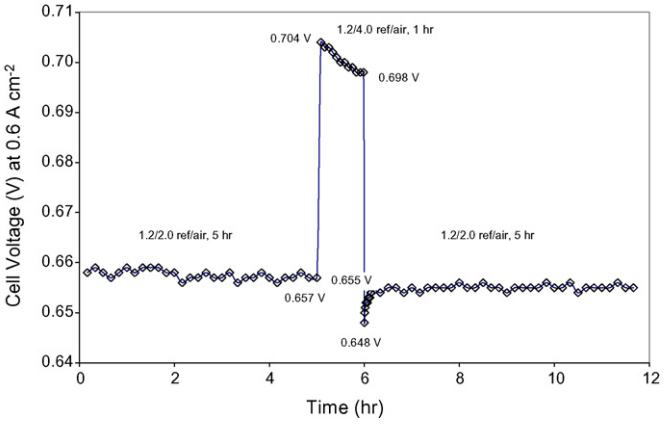

Fig. 11. Effect of increasing air stoichiometry from 2.0 to 4.0 on performance of a new single cell. Premixed fuel gas with 10 ppm CO, 49% H_2, 17% CO_2, balanced by N_2; 100% RH; 65 °C cell temperature; 2% air bleed; 0.6 A cm^{-2} load.

The different behaviors between new and aged cells make us believe that MEA aging reduces its hydrophobicity, which in turn leads to an increase in the mass transport resistance. The reduction in hydrophobicity of both electrodes and GDLs due to component aging is a well-observed phenomenon [5,36].

4. Conclusions

A systematic investigation confirmed that the "saw-tooth" behavior observed during fuel cell shutdown and restart cycles was caused primarily by the removal of excess water from a fuel cell by the reactant flows under OCV during the cool down and warm up periods. Although catalyst oxidation state change and surface cleansing could result in similar behaviors, they did not show any significant contributions to the "saw-tooth" behavior under our experimental conditions.

Acknowledgments

The authors are grateful to Ms. Cynthia Mahoney White, Mr. Daniel Beaty, and Mr. Jeffrey Boyer for their critical review of this article.

References

[1] F. Barbir, System design for stationary power generation, in: W. Vielstich, A. Lamm, H.A. Gasteiger (Eds.), Handbook of Fuel Cells — Fundamentals Technology and Applications, vol. 4, John Wiley & Sons, 2003, pp. 684–713.
[2] A.S. Feitelberg, J. Stathopoulos, Z. Qi, C. Smith, J.F. Elter, J. Power Sources 147 (2005) 203–207.
[3] P.J. Ferreira, G.J. la O', Y. Shao-Horn, D. Morgan, R. Makharia, S. Kocha, H.A. Gasteiger, J. Electrochem. Soc. 152 (2005) A2256.
[4] P. Piela, C. Eickes, E. Brosha, F. Garzon, P. Zelenay, J. Electrochem. Soc. 151 (2004) A2053.
[5] J. Xie, D.L. Wood III, D.M. Wayne, T.A. Zawodzinski, P. Atanassov, R.L. Borup, J. Electrochem. Soc. 152 (2005) A104.
[6] J. Aragane, T. Murahashi, T. Odaka, J. Electrochem. Soc. 135 (1988) 844.
[7] M.S. Wilson, F.H. Garzon, K.E. Sickafus, S. Gottesfeld, J. Electrochem. Soc. 140 (1993) 2872.
[8] J. St-Pierre, D.P. Wilkinson, S. Knight, M. Bos, J. New Mater. Electrochem. Syst. 3 (2000) 99.
[9] J.A.S. Bett, K. Kinoshita, P. Stonehart, J. Catal. 41 (1976) 124.
[10] D.A. Stevens, J.R. Dahn, Carbon 43 (2005) 179.
[11] D.A. Stevens, M.T. Hicks, G.M. Haugen, J.R. Dahn, J. Electrochem. Soc. 152 (2005) A2309.
[12] J.M. Thomas, Carbon 8 (1970) 413.
[13] L.L. Van Dine, M.M. Steinbugler, C.A. Reiser, G.W. Scheffler, US Patent No. 6,514,635 (2003).
[14] D.A. Condit, R.D. Breault, US Patent No. 6,635,370 (2003).

[15] T.A. Bekkedahl, L.J. Bregoli, R.D. Breault, E.A. Dykeman, J.P. Meyers, T.W. Patterson, T. Skiba, C. Vargas, D. Yang, J.S. Yi, US Patent No. 6,913,845 (2005).
[16] C.R. Reiser, L. Bregoli, T.W. Patterson, J.S. Yi, J.D. Yang, M.L. Perry, T.D. Jarvi, Electrochem. Solid-State Lett. 8 (2005) A273.
[17] H. Tang, Z. Qi, M. Ramani, J.F. Elter, J. Power Sources 158 (2006) 1306–1312.
[18] S.D. Gottesfeld, US Patent No. 4,910,099 (1990).
[19] R.M. Darling, J.P. Meyer, J. Electrochem. Soc. 105 (2003) A1523.
[20] A.K.N. Reddy, M.A. Genshaw, J.O'M. Bockris, J. Chem. Phys. 48 (1968) 671.
[21] P.N. Ross, N.M. Markovic, J. Electrochem. Soc. 137 (1990) 3368.
[22] M. Teliska, V.S. Murthi, S. Mukerjee, D.E. Ramaker, J. Electrochem. Soc. 152 (2005) A2159.
[23] C. Clay, S. Haq, A. Hodgson, Phys. Rev. Lett. 92 (2004) 46102.
[24] A. Pozio, L. Giorgi, E. Antolini, E. Passalacqua, Electrochim. Acta 46 (2000) 555.
[25] H. Massong, H. Wang, G. Samjeske, H. Baltruschat, Electrochim. Acta 46 (2000) 701.
[26] Z. Qi, C. He, A. Kaufman, Electrochem. Solid-State Lett. 4 (2001) A204.
[27] D.-T. Chin, P.D. Howard, J. Electrochem. Soc. 133 (1986) 2447.
[28] M. Mathieu, M. Primet, Appl. Catal. 9 (1984) 361.
[29] R. Mohtadi, W.-K. Lee, S. Cowan, J.W. Van Zee, M. Murthy, Electrochem. Solid-State Lett. 6 (2003) A272.
[30] G. Pourcelly, A. Oikonomou, C. Gavach, J. Electroanal. Chem. 287 (1990) 43.
[31] M. Watanabe, Y. Satoh, C. Shimura, J. Electrochem. Soc. 140 (1993) 3190.
[32] T.E. Springer, M.S. Wilson, S. Gottesfeld, J. Electrochem. Soc. 140 (1993) 3513.
[33] Z. Qi, A. Kaufman, J. Power Sources 109 (2002) 469.
[34] T. Abe, H. Shima, K. Watanabe, Y. Ito, J. Electrochem. Soc. 151 (2004) A101.
[35] H. Xu, Y. Song, H.R. Kunz, J.M. Fenton, J. Electrochem. Soc. 152 (2005) A1828.
[36] T. Kinumoto, K. Takai, Y. Iriyama, T. Abe, M. Inaba, Z. Ogumi, J. Electrochem. Soc. 153 (2006) A58.